Production of γ, π^0 and η at Large Transverse Momenta*

J. Biel, C. Bromberg, B. Brown, C. Chandlee, S. Cihangir, S. Cooper, T. Ferbel, D. Garelick, G. Glass, M. Glaubman, S-R. Han, K. Heller, S. Hossain, J. Huston, A. Jonckheere, J. LeBritton, R. A. Lewis, F. Lobkowicz, M. Marshak, M. McLaughlin, C.A. Nelson, Jr., E. Peterson, E. Pothier, J. Povlis, K. Ruddick, P. Slattery, G. A. Smith, M. Shupe
Fermilab-Michigan State-Minnesota-Northeastern-Rochester Collaboration†

CONF-820718--3

DE82 018754

ABSTRACT

A measurement of direct photon production, as well as of π^0 and η meson production, has been performed at Fermilab. Data were taken for 200 GeV/c p and π^+ incident on Be, C and Al targets. The ratio of γ/π^0 inclusive cross sections is presented for transverse momenta between 2 and 5 GeV/c.

*Submitted to the XXIst International Conference on High Energy Physics, Paris, July 1982.

†Research supported by the Department of Energy and the National Science Foundation.

This report presents preliminary results from Fermilab experiment E629, whose purpose was to measure the production of single photons at large p_T, and to determine whether liquid argon calorimeters could be used at the high beam rates required to probe large-p_T phenomena at fixed-target machines.

The overall arrangement for the experiment is shown in Fig. 1. The incident positive beam (85% p, 15% π^+) of 200 GeV/c momentum was defined by several scintillation counters, including one precision XY measuring hodoscope. Two Cerenkov counters (not shown) in the beam line were used to tag each particle as either a pion or a proton. The targets (Carbon, Beryllium or Aluminum) were subdivided into two segments separated by 25 cm; two sets of counters downstream of the target, situated just outside of the beam, were used to define an interaction in the target. Various veto and halo counters suppressed triggers from the halo around the beam; in addition, a wall of scintillation counters ("veto wall"), that shadowed our electromagnetic shower detector, was used to suppress triggers from particles produced by interactions upstream of the target.

Charged particles emitted to one side of the target were detected in a set of proportional wire chambers (PWC); these also identified the target segment in which the interaction took place. Photons were detected using a Liquid Argon Calorimeter (LAC), which we employed in a previous experiment.[1] The LAC is composed of a stack of 2 mm lead plates, separated by 2 mm gaps of liquid argon from copper-clad G-10 boards, which serve as readout boards. The sensitive area of the LAC is 1.4 m × 0.81 m. The LAC has alternate layers of X and Y readout strips; the strips are 1.27 cm wide. There are no U or V view readout strips; the correlation between the X and the Y view is made on the basis of energy matching. The two views provide independent energy measurements of a shower; the correlation algorithm finds for each X-view

of the shower the Y-view which most closely matches its energy. Details of the LAC performance are discussed elsewhere,[1] here we mention only those features which directly affect the present experiment.

The energy resolution for photons and electrons during the experiment was $14\%/\sqrt{E(GeV)}$, with an effective low-energy noise level of $\sim$500 MeV/photon that had to be added in quadrature. The rms position resolution for electrons was less than 1 mm. The overall resolution achieved during calibration was better by a factor $\sim$1.5. Thus, it appears that pedestal drifts, reconstruction algorithms and other systematics contribute substantially to the effective resolution.

The LAC had a total thickness of 25 radiation lengths, and presented 0.9 absorption lengths to pions. The readout was subdivided so that the front and the back 12.5 r.l. were read out separately. This helped in discriminating against hadrons. In Fig. 2a we show the probability that a hadron deposits more than a certain fraction of its total energy as visible energy E_{VIS} in the LAC. Figure 2b shows the probability that a hadron deposits less than a certain fraction of its visible energy in the back part of the LAC when the total visible energy E_{VIS} (front and back) is at least 10% of the total hadron energy. For comparison purposes, the same distribution is also shown for electrons. A cut in E_{BACK}/E_{VIS} of 0.2 eliminates 90% of all hadrons, but cuts the photon signal by only 10%.

The LAC provided the main trigger for the experiment. The total transverse momentum of a photon is given by $p_T = p_\gamma \sin\theta = E_\gamma \sin\theta$, where θ is the laboratory angle between the beam direction and the outgoing direction of the photon. We implemented a "global p_T" requirement by adding all the X-strip energies, suitably attenuated to achieve a global p_T. The Y-strips, appropriately attenuated, were also added into the trigger so that an event

passed the threshold if its total p_T was $\gtrsim$ 2.5 GeV/c. In addition, deposition of a "local p_T" of $\gtrsim$ 0.8 GeV/c was required in three neighboring X-strips to satisfy the trigger. The latter served to suppress triggers by multi-π^o jets in which every π^o had a small p_T value (i.e., $\lesssim$ 1.6 GeV/c).

The efficiency of the trigger threshold was monitored by collecting a fraction of the data with a lower threshold value for the global p_T, and latching information for those events that satisfied the normal global-p_T requirement. Figure 3 shows the fraction of events passing the global p_T trigger for data in which either a single π^o or a single photon appeared in the LAC. The threshold curve for π^o data appears to be consistent with that obtained for triggers with only single showers.

The average photon multiplicity in the LAC for all data is 4.4 photons/event. Most of these events correspond to multiphoton jets. When one of the photons is required to have a p_T > 2.5 GeV/c, the average photon multiplicity drops to 2.1 photons event. Any measurement of direct single-photon production must include a study to ascertain π^o, η, ω,...yields; this is because, for each meson, there always exists a region of the phase space volume where one of the photons from the meson decay has nearly the full hadron momentum, while the other photons have low momentum and can either escape detection or miss the detector altogether. Figure 4a displays the invariant mass distribution of all two-photon events in the π^o and the η mass regions. Figure 4b shows the same distributions for multiphoton events; only those 2γ combinations are plotted whose total p_T exceeds 2.5 GeV/c. Clear π^o and η peaks are apparent in Fig. 4. (A small ω signal has also been detected at large p_T.) The degree to which we understand the π^o and, to a lesser extent, the η^o and ω data, determines the confidence that we can assign to any direct photon excess that we observe. A particularly crucial

test of our understanding of the background is contained in a comparison between the observed and expected decay distributions for π^o and η signals. In particular, the asymmetry in the laboratory energies of the two photons from π^o or from η decays $[(E_1-E_2)/(E_1+E_2)]$, equal to the cosine of the helicity decay angle of the photon (with respect to the $\pi^o(\eta)$ direction), should be isotropically distributed between 0.0 and 1.0 for spin-zero objects.

Figure 5 presents the asymmetry distribution of both π^o and η mesons observed in the detector. Also shown is the asymmetry distribution of the two-photon background near the two meson masses. The background asymmetry distribution peaks at large asymmetry; this is because most background events consist of one high energy photon and one rather soft one. In contrast, the π^o and η events tend to be lost at large asymmetries. The smooth curves are our Monte Carlo predictions for the background-subtracted π^o and η signals, which clearly agree with the data. The agreement between the data and Monte Carlo is particularly important here because events which are missing at large asymmetries in Fig. 5 are just the ones that contribute to the background in the single-photon events.

The A-dependence of the inclusive π^o and η yield above a p_T of 2.5 GeV/c in p-A data is shown in Fig. 6; the yield exhibits an A^α dependence. The values of α for π^o production and η production by both protons and pions are given in Table I. Above a p_T of 2.5 GeV/c, none of these values show a significant variation with p_T. The value of α for π^o production is similar to that measured by the Chicago-Princeton group for charged pion production[2]; although statistics are poor, the η yield may have a somewhat steeper A-dependence.

The p_T dependence of π^o production in pp collisions is substantially steeper than in πp collisions.[3] This interesting result, can, in principle,

Table I. A^{α}-dependence of π^{o} and η production

Reaction	α
$pN \rightarrow \pi^{o}X$	1.09 ± 0.09
$pN \rightarrow \eta X$	1.14 ± 0.21
$\pi^{+}N \rightarrow \pi^{o}X$	1.0 ± 0.3
$\pi^{+}N \rightarrow \eta X$	1.8 ± 0.6

be used to shed light on whether at large p_T, hadrons in nuclei are produced through elementary interactions rather than, for example, through multi-step rescattering processes. Our data, shown in Fig. 7, indicate the same trend for the ratio of π^{o} production by protons and pions on nuclear targets, as was observed earlier on hydrogen.[3] Consequently, because rescattering would tend to change the shape of the p/π production ratio with increasing nuclear size, it appears that multi-step processes do not play a major role in the enhancement of the π^{o} yield at large p_T on nuclei, at least out to $p_T \sim 4$ GeV/c.

We now turn our attention to single photon production. For $p_T > 3.5$ GeV/c, 85% of the large p_T photons are isolated, i.e., no other photons of $\geq$ 1 GeV accompany them in the detector. For π^{o} production the situation is not as dramatic, but even here less than one-third of the π^{o} mesons are accompanied by additional photons.

Many of the single-photon events at large p_T correspond to random coincidences between a beam interaction in the target and a photon (or hadron) produced by an interaction further up the beam line. Although such events are suppressed by the veto wall shown in Fig. 1, the suppression is not total. However, two different cuts, one on the timing and one of the direction of the incident particle as measured by the LAC, can be used to reject such background events.

The LAC samples the shower in both its front and back sections. As illustrated in Fig. 8a, the quantity ΔX_B is the difference between the actual shower position in the back and that predicted from the front, assuming that the photon originated from the target. In a scatter plot of ΔX_B against the transverse position of the shower in the front of the LAC, shown in Fig. 9b, two distinct bands of events can be seen; one with $\Delta X_B \simeq 0$, corresponding to showers originating in the target, and another which identifies showers from upstream sources.[4] From the scatter plot, we conclude that we can measure the direction of incident showers to ± 30 mr (rms).

The signals from each of the X-strips of the LAC, and from some of the Y-strips were fed to time-to-digital pulse converters. In Fig. 9 we show the timing distribution of all single showers for several ranges of p_T. While for the moderate p_T values nearly all LAC signals are in time with the trigger pulse from the interaction in the target, at large p_T most of the LAC signals are out of time. Fixed delays in the LAC amplifiers required that the decision to accept or reject a trigger had to occur within 250 ns of the arrival of photons at the LAC. Because of this and because of intrinsic delay in the formation of the veto, particles in the halo that arrived >50 ns after t=0 could not be vetoed. Note that despite the rather long rise time of ∿200 nsec for the LAC pulse, timing accuracy to ±6 nsec can be achieved; at large p_T, one can clearly see the r.f. beam structure with a 19 nsec repetition rate. In the distributions shown in Fig. 9, events surviving the direction cut are shown cross-hatched. At low p_T, the two cuts, namely, directionality and timing, tend to reject the same events and thus can be used to check each other; at larger p_T, both criteria are needed to obtain a clean signal.

The inclusive γ/π^0 ratio, shown separately for pC and π^+C data, with all cuts applied, is shown as a function of p_T in Fig. 10. The data have been integrated over ∿1.2 units of rapidity, centered at $y_{cm} = 0$. The cross-

hatched band is the Monte Carlo prediction for the background expected from observed π^o, η, η' and ω decays; it contains corrections for hadron interactions in the LAC, effects due to trigger biases and reconstruction inefficiency. Changing various cuts in the data (e.g., asymmetry, detector aperture), or modifying the assumptions about threshold behavior or the rapidity dependence of mesons that miss the LAC, affects the estimate of the background. The widths of the bands in Fig. 10 reflect the uncertainty in the parameterization of these backgrounds. For p_T less than 3 GeV/c our data are consistent with essentially no direct photon signal ($\gamma/\pi^o \lesssim 5\%$); a definite signal in both π^+C and pC data can be discerned at larger p_T. The results for π^+ and p are consistent with each other as well as with ISR data.[5] The magnitude of the effect at low p_T values is not as large as reported previously by another Fermilab experiment.[6] Our results, consequently, favor a lack of energy dependence in the γ/π^o yield at fixed p_T.

We wish to thank Drs. A. Brenner, N. Gelfand, P. Koehler, L. Lederman, E. Malamud, J. Peoples and T. Yamanouchi at Fermilab for their support of our experiment.

REFERENCES

1) C. A. Nelson et al., Nucl. Instrum. Methods (to be published).

2) D. Antreasyan et al., Phys. Ev. D19, 764 (1979).

3) G. Donaldson et al., Phys. Rev. Lett. 36, 1110 (1976). See also N. Giokaris et al., Phys. Rev. Lett. 47, 1690 (1981), for a comparison with charged pion production on hydrogen.

4) The two gaps in the distribution are due to dead strips in the back of the LAC.

5) M. Diakonou et al., Phys. Lett. 91B, 296 (1980) and E. Anassontzis et al., Z. Phys.C. (to be published), CERN-EP/82-26 (1982).

6) R. Baltrusaitis et al., Phys. Lett. 88B, 372 (1979.

FIGURE CAPTIONS

Fig. 1 Experimental setup.

Fig. 2 (a) Integral pulse height distribution in LAC for hadrons.
(b) Integral distribution of E_{BACK}/E_{VIS} for hadrons and electrons.

Fig. 3 Trigger efficiency of the global p_T requirement for single π^o and single photons.

Fig. 4 Two-photon mass distribution.
(a) Two photons hit LAC.
(b) Three or more photons hit LAC.

Fig. 5 Asymmetry distribution for $\pi^o(\eta) \rightarrow 2\gamma$ decays. The asymmetry distribution of the backgrounds near the two peaks are also shown. The curves are Monte Carlo calculations.

Fig. 6 The dependence of the inclusive π^o and η yield on nuclear size for $p_T > 2.5$ GeV/c. (Integrated over $\sim$1.2 units of rapidity, centered at $y_{cm} \approx 0$.)

Fig. 7 The ratio of π^o production by protons and π^+ as a function of p_T, for several targets. The hydrogen data are from Ref. 3.

Fig. 8 The directionality cut:
(a) definition of ΔX_B;
(b) for events with single showers, scatter plot of ΔX_B vs. transverse position in LAC.

Fig. 9 Timing distributions for all single showers for several intervals in p_T. The shaded events survive the directionality cut.

Fig. 10 The observed ratios γ/π^o. The lower shaded bands indicate the backgrounds due to misidentified meson decays and other sources. The additional band in the pC data corresponds to the γ/π^o signal reported by Anassontzis et al. (Ref. 5) for pp data at $\sqrt{s} = 31$ GeV.

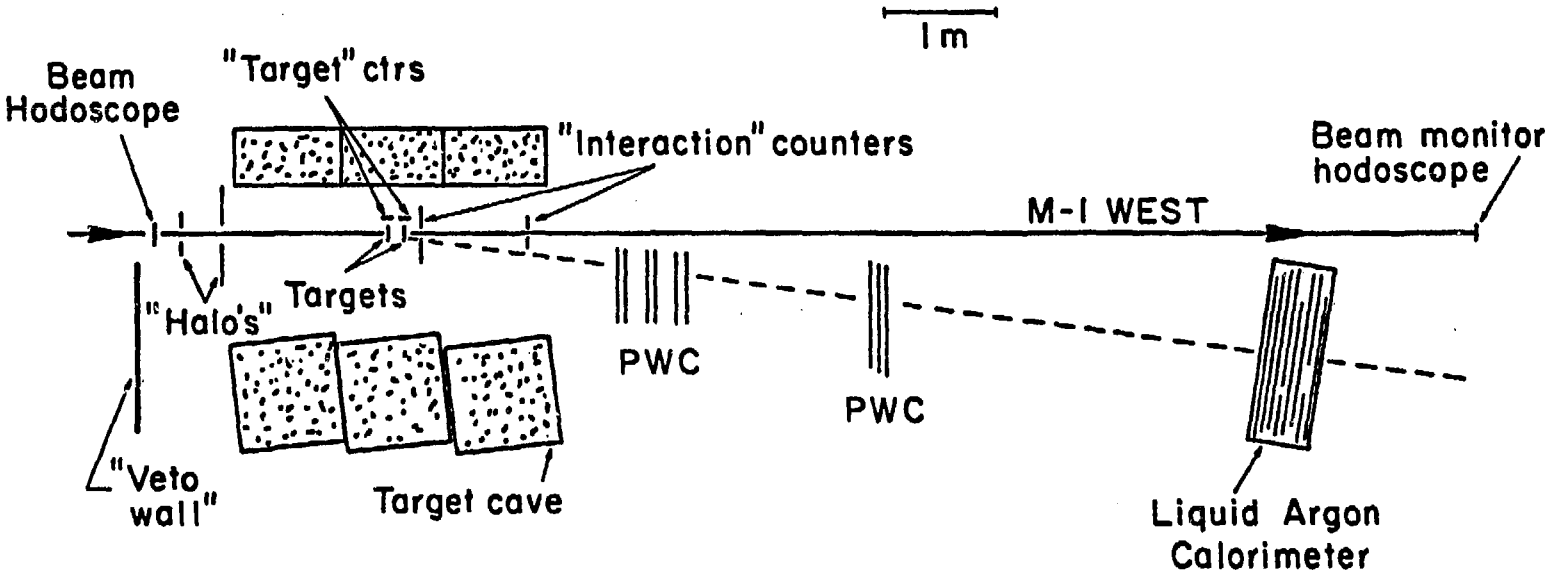
1 m
Beam Hodoscope
"Target" ctrs
"Interaction" counters
Beam monitor hodoscope
M-1 WEST
"Halo's"
Targets
PWC
PWC
"Veto wall"
Target cave
Liquid Argon Calorimeter

Fig. 1

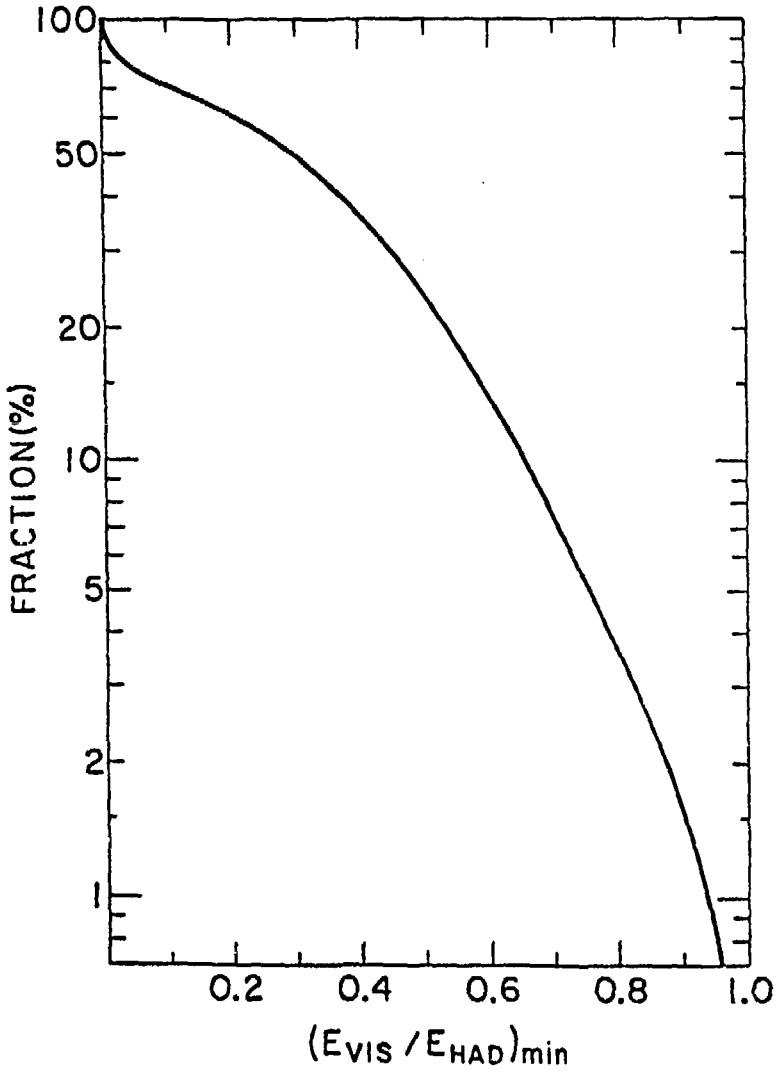
100
50
20
10
5
2
1
FRACTION(%)
0.2
0.4
0.6
0.8
1.0
$(E_{VIS}/E_{HAD})_{min}$

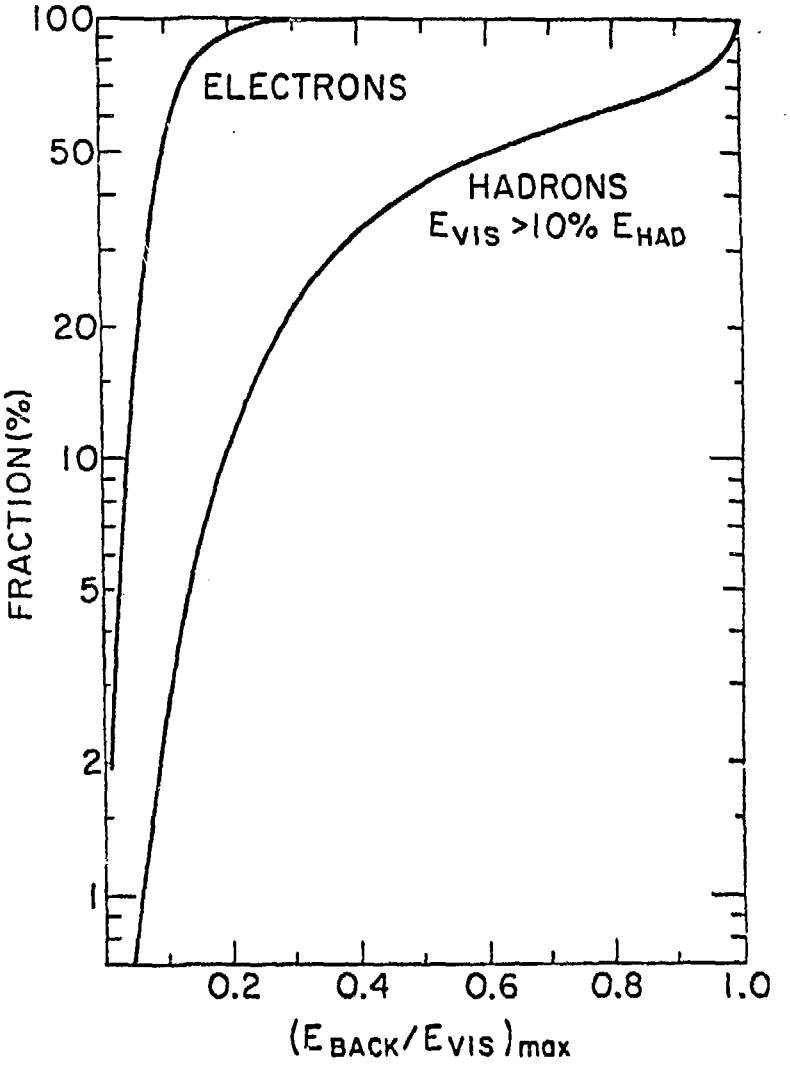
100
50
20
10
5
2
1
FRACTION(%)
ELECTRONS
HADRONS
$E_{VIS} > 10\% E_{HAD}$
0.2
0.4
0.6
0.8
1.0
$(E_{BACK}/E_{VIS})_{max}$

Fig. 2

TRIGGER EFFICIENCY – π^0

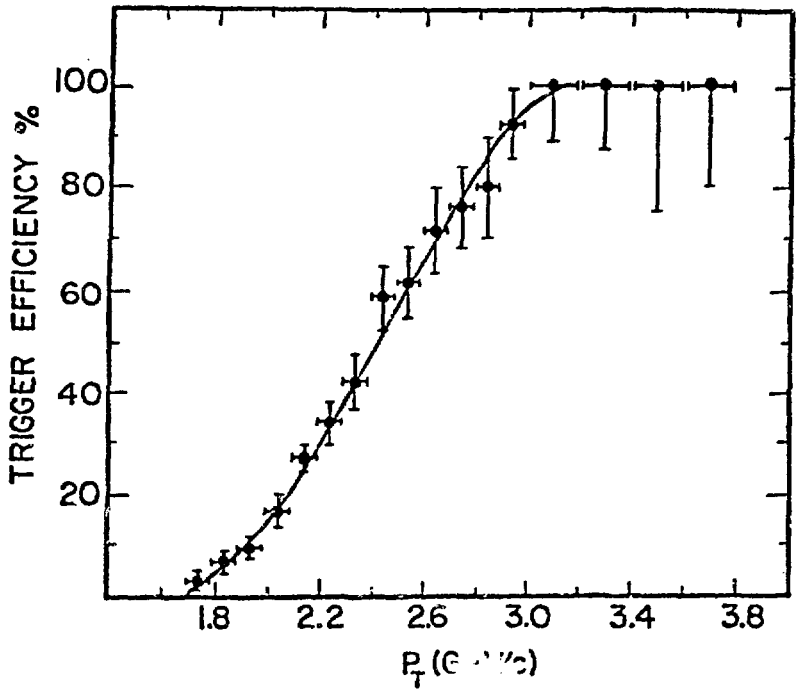

TRIGGER EFFICIENCY — SINGLE SHOWER

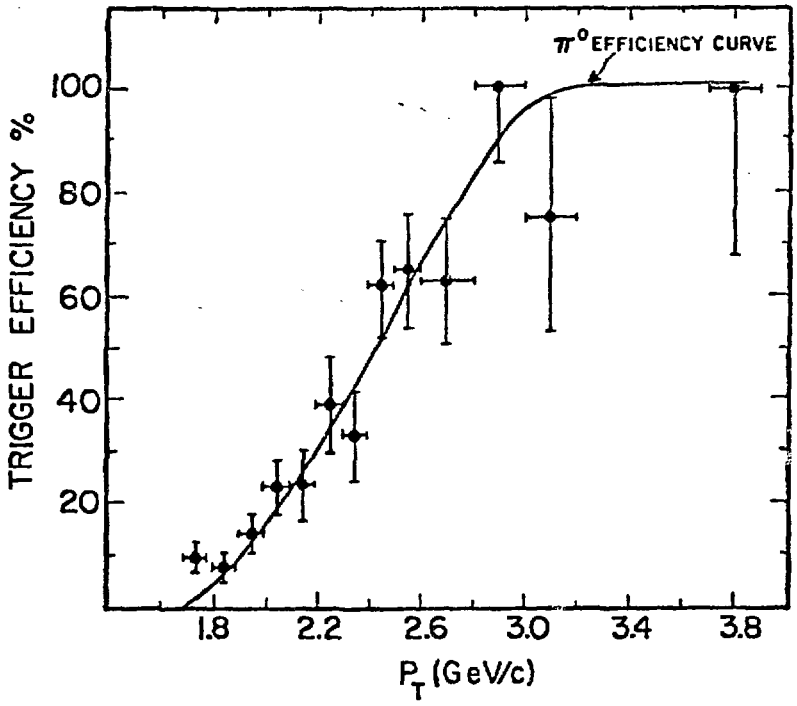

Fig 3

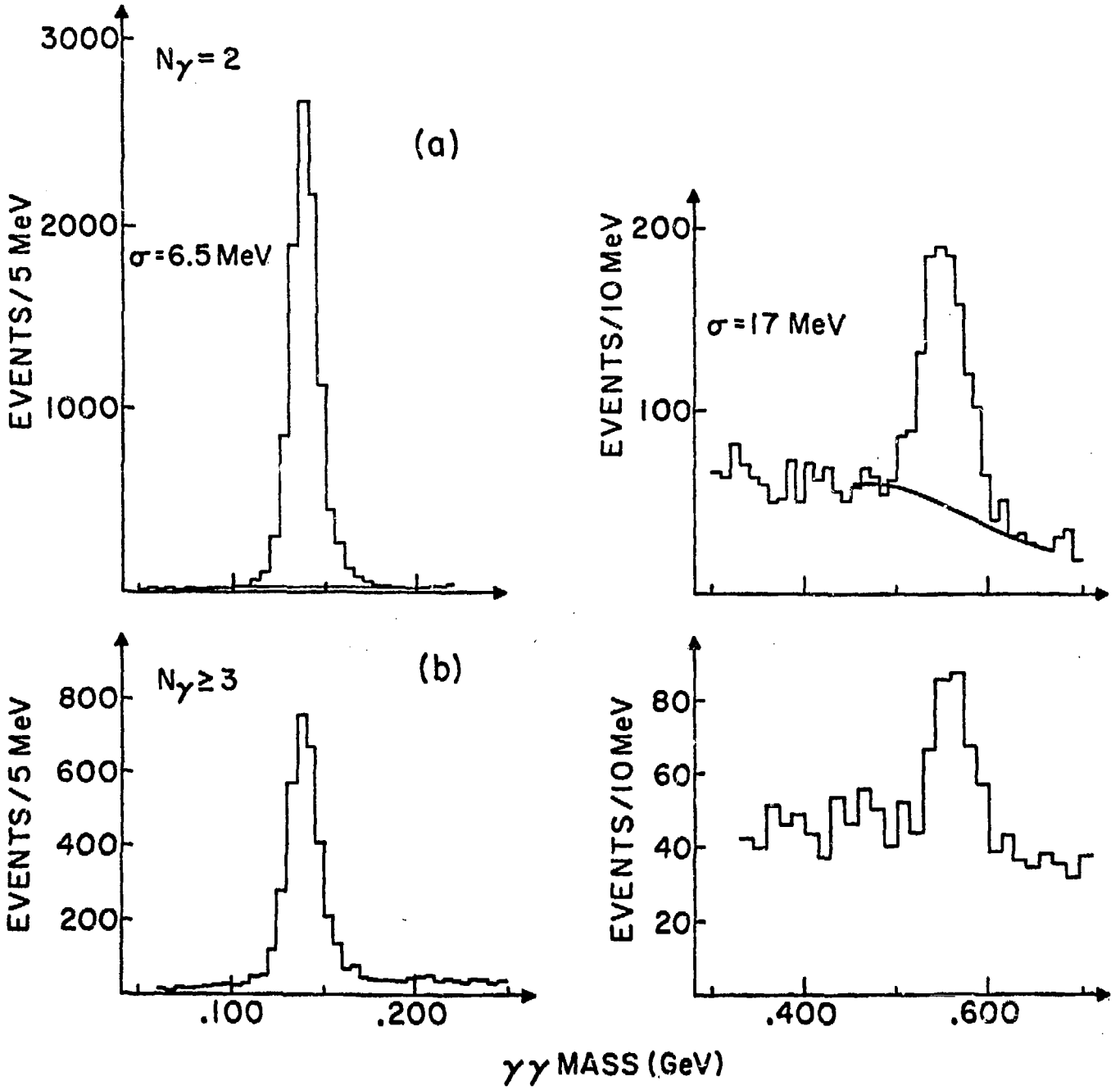
3000
2000
1000
EVENTS/5 MeV
$N_\gamma = 2$
(a)
$\sigma = 6.5$ MeV
200
100
EVENTS/10 MeV
$\sigma = 17$ MeV
800
600
400
200
EVENTS/5 MeV
$N_\gamma \geq 3$
(b)
80
60
40
20
EVENTS/10 MeV
.100
.200
.400
.600
$\gamma\gamma$ MASS (GeV)

Fig. 4

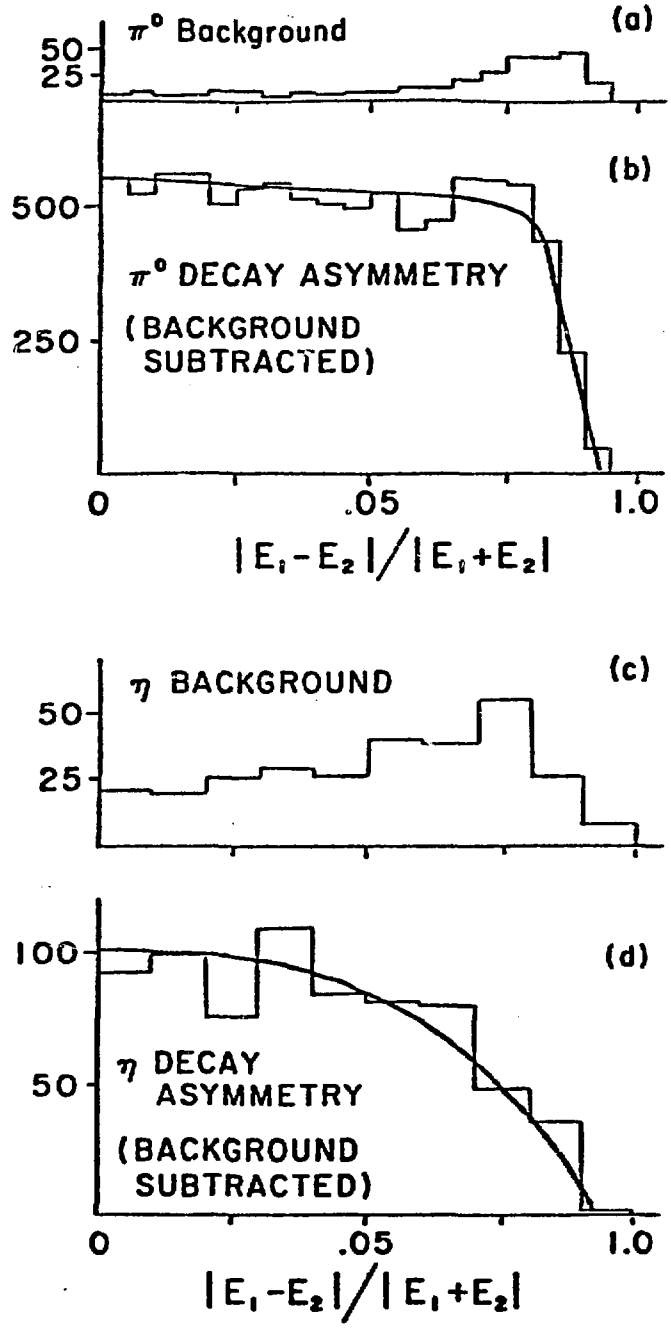
π° Background
(a)
50
25
(b)
500
250
π° DECAY ASYMMETRY
(BACKGROUND
SUBTRACTED)
0
.05
1.0
|E₁-E₂|/|E₁+E₂|
η BACKGROUND
(c)
50
25
100
(d)
50
η DECAY
ASYMMETRY
(BACKGROUND
SUBTRACTED)
0
.05
1.0
|E₁-E₂|/|E₁+E₂|

Fig 5

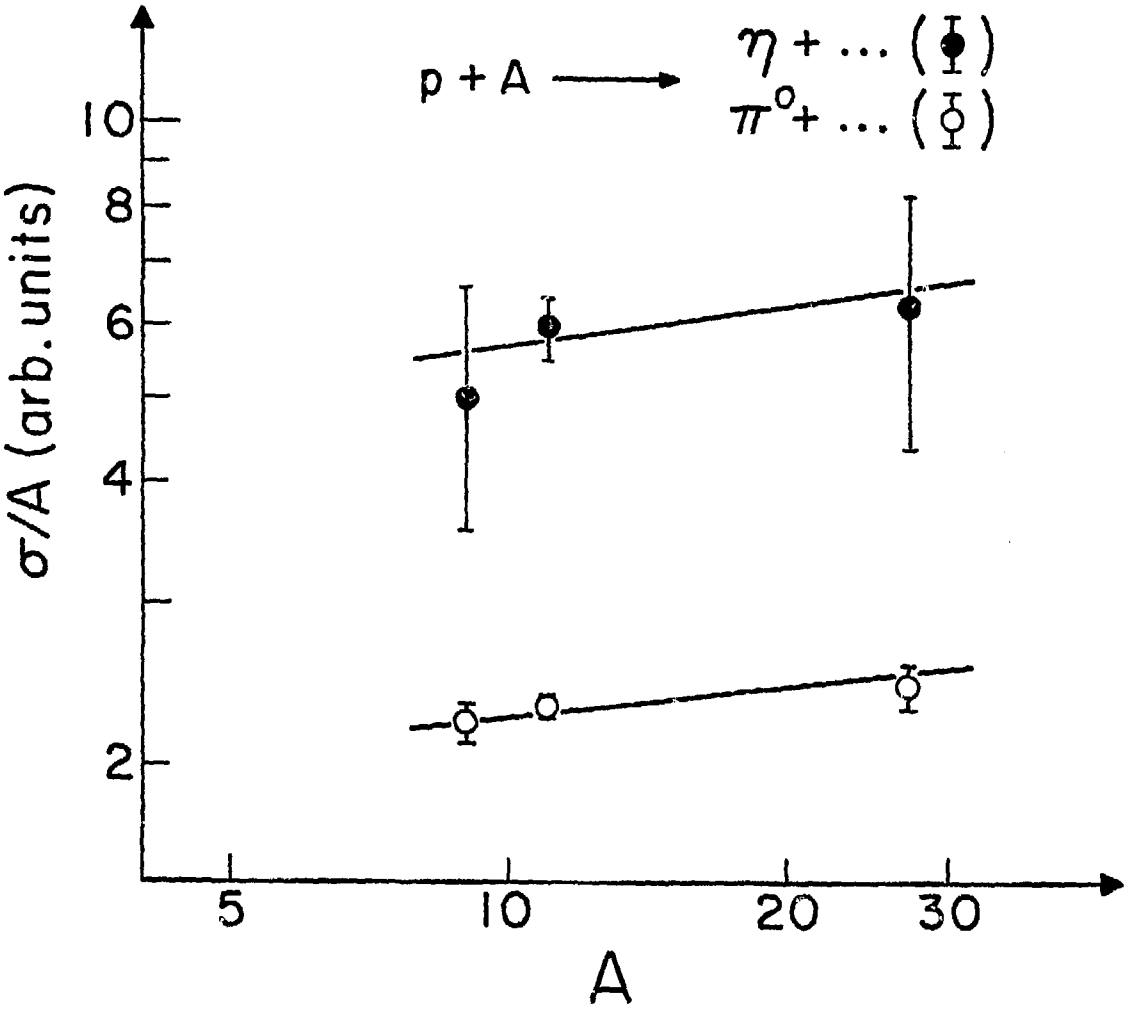

Fig. 6

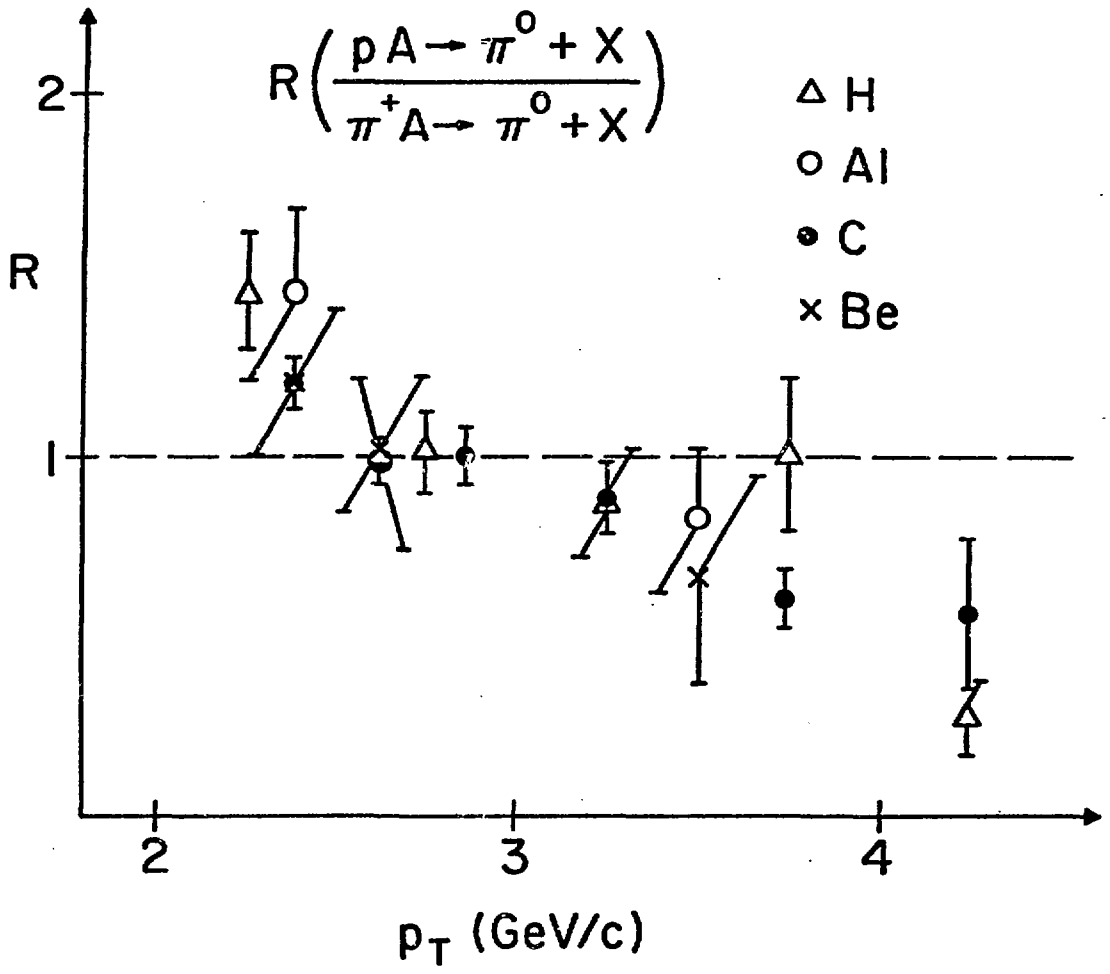

Fig 7

$$\Delta X_B = \frac{T_{LAC}}{D_{LAC}} (X_F - X_0)$$

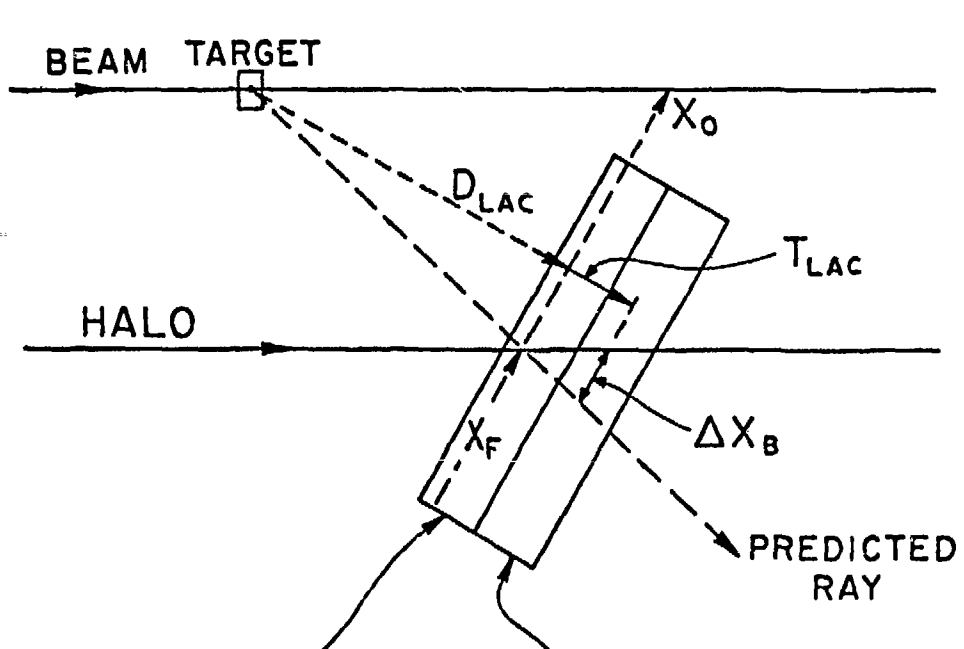

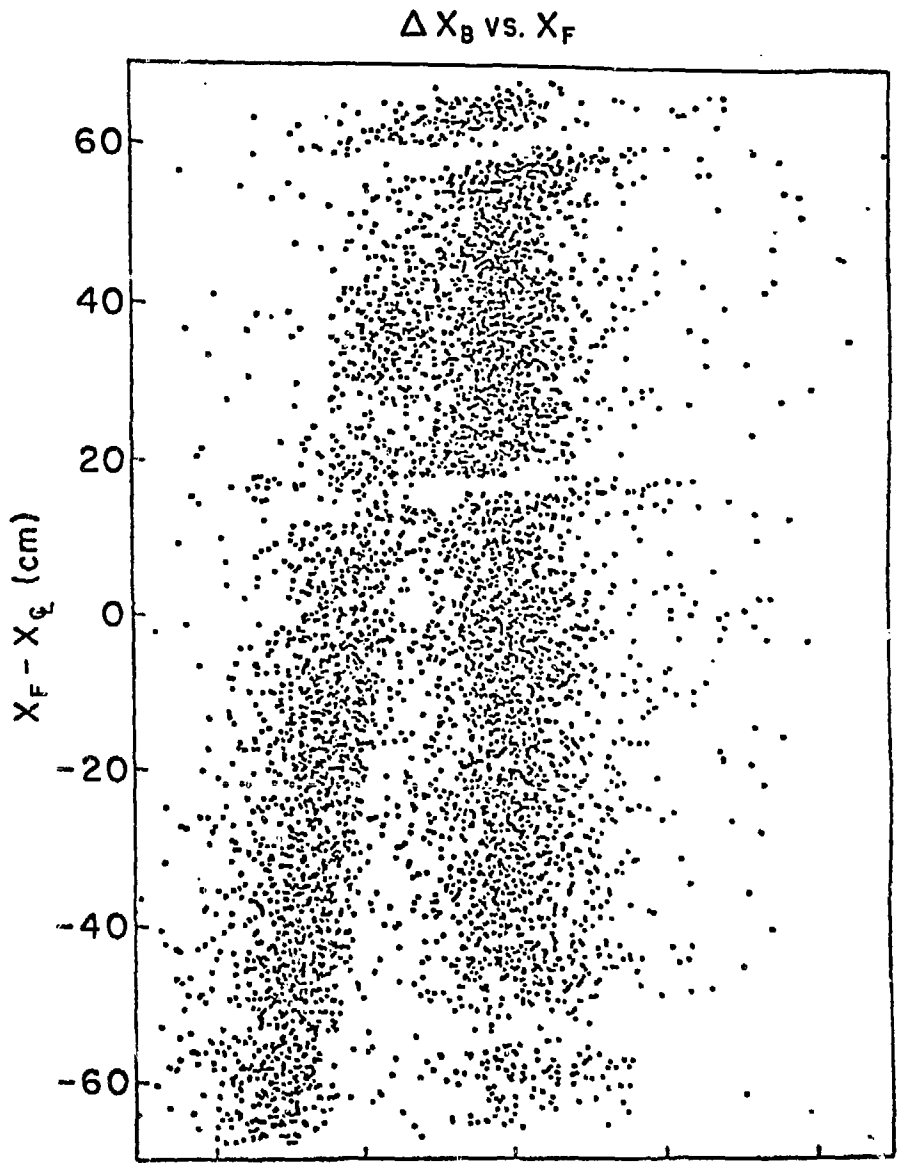

Fig. 8

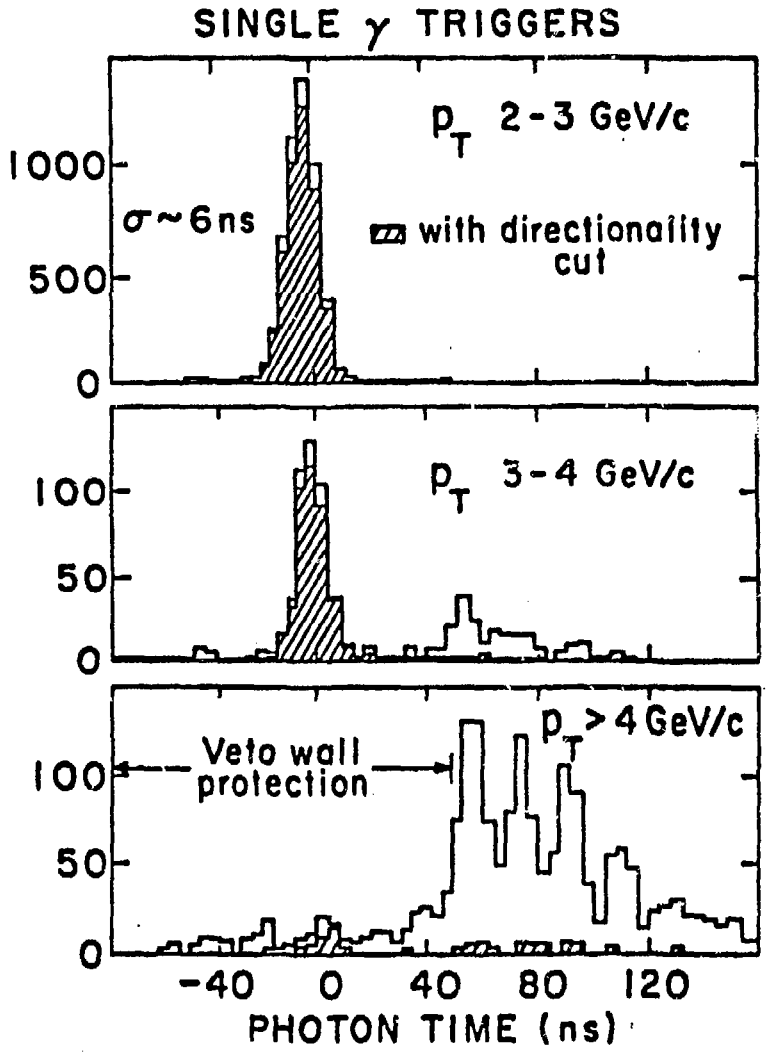
SINGLE γ TRIGGERS
1000
500
0
σ~6ns
p_T 2-3 GeV/c
with directionality cut
100
50
0
p_T 3-4 GeV/c
100
50
0
Veto wall protection
p_T > 4 GeV/c
-40
0
40
80
120
PHOTON TIME (ns)

Fig. 9

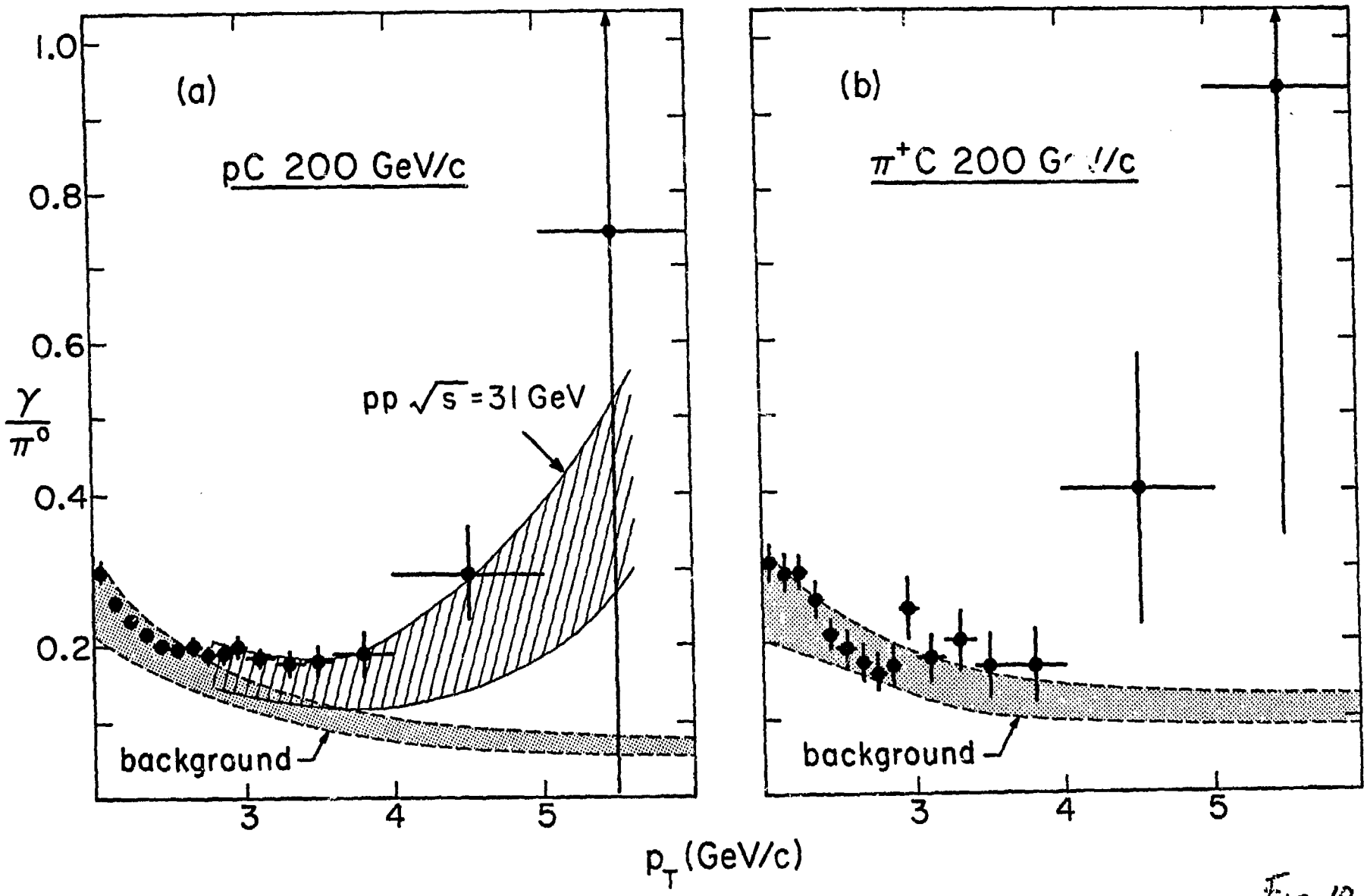
(a)
pC 200 GeV/c
pp $\sqrt{s}$ = 31 GeV
background
(b)
π^+C 200 G
/c
background
$\frac{\gamma}{\pi^0}$
1.0
0.8
0.6
0.4
0.2
3
4
5
p_T (GeV/c)

Fig. 10